Ab initio study on the electronic and optical properties of B-doped ZnO

DEPING XIONG*, MIAO HE, WEI ZHANG, WEIREN ZHAO, QU WANG, ZUYONG FENG
School of Physics and Optoelectronic Engineering, Guangdong University of Technology, Guangzhou, 510006, China

The electronic and optical properties of B-doped ZnO were studied by ab initio calculation. The calculated formation energies reveal that the structure (labeled as $B_{s(Zn)}$) of boron atom substituting zinc atom forms easily compared to the other B-doped ZnO structures, and the preparation of high boron concentration in B-doped ZnO is difficult. For $B_{s(Zn)}$ structure with different boron concentration, the Fermi energy is located in the conduction band, indicating a typical n-type semiconductor material, the band-gap decreases with boron concentration increasing. In the range of 400nm-1200nm, the transmittance spectra shows the transmittance of ZnO is larger than 90%, the transmittance decreases with the incorporation of boron (6.25at.%-18.75at.%), at wavelength shorter than 300nm, the transmittance of B-doped ZnO is higher than that of ZnO.

(Received May 7, 2018; accepted February 12, 2019)

Keywords: Ab initio calculation, Electronic structure, Optical properties, B-doped ZnO

1. Introduction

Transparent conductive oxides (TCOs) are important in fabricating optoelectronic devices, such as display devices [1], solar cells [2-4], and light emitting diodes [5,6]. Among these compounds, III-doped ZnO is becoming a potential candidate to substitute indium tin oxide (ITO) as transparent conducting films due to its competitive electronic and optical properties. In recent years, Al or Ga-doped ZnO have received particular attention and been widely studied [7-10]. For Al-doped ZnO (AZO), when Al concentration exceeds 3at.%, interstitial Al atoms are easily formed, the resistivity of Al-doped ZnO doesn't decrease continuously[11]. Ga-doped ZnO (GZO) is believed to have considerable potential due to its low Madelung energy and ionic radius between Ga^{3+} (0.62 Å) and Zn^{2+} (0.74 Å) [12]. Similarly, B-doped ZnO (BZO) also show promising features in high transmittance and low resistivity[13], are regarded as an alternative to ITO films used in optoelectronic fields. Li Gao et al.[14] deposited B-doped ZnO films on glass substrates by radio frequency magnetron sputtering method, the films show high average optical transmission (≥80%) and low resistivity ($9.2\times10^{-3}\Omega\cdot cm$). Y.F.Wang et al.[15] deposited B-doped ZnO films using pulsed direct-current magnetron sputtering, the films annealed at 450°C in an Ar atmosphere had the lowest resistivity of 2.39×10^{3} Ω·cm. On the other hand, however, it is still unclear in some properties of B-doped ZnO, due to the small ion radius, boron can act as either substituted atom or interstitial one in ZnO lattice[16], in addition, the relationship of boron concentration on the properties of B-doped ZnO was seldom reported compared to Ga or Al-doped ZnO [7,10,13,17]. Therefore, it is necessary to study these effects, and this is also the purpose of the paper.

From a theoretical perspective, the properties of III-doped ZnO were generally studied based on the density functional theory (DFT), it was found that the calculated band-gap of ZnO is much smaller than the experimental values [14,18], the result of underestimation is the natural limitation decided by DFT[19]. The DFT+U approach attempts to make up for the limitation by using an orbital dependent term added to the DFT potential. To improve the value of band-gap, recently many theoretical researches have studied the impact of U parameter on the properties of ZnO, and the correct band-gap for ZnO can be obtained by this way [20,21]. Therefore, we adopted the DFT+U method in this study, four possible B-doped ZnO structures were considered, they are the substitution of boron for zinc or oxygen, and interstitial boron in a tetrahedron or in an octahedron. By comparing with the formation energies, we identified the most possible structure of four types of B-doped ZnO structures, then we investigated the physical properties of B-doped ZnO with this structure, the analysis was carried out using boron concentrations of 6.25at.%, 12.5at.%, and 18.75at.%, respectively. As far as we know, presently few studies ever focused on the effects of boron concentration on the properties of B-doped ZnO.

2. Calculation methods

ZnO has wurtzite structure, the lattice constants are *a*

$=b$=3.249Å and c=5.206 Å[22]. In this study we employed a 2×2×2 supercell of ZnO containing 32 atoms, and four types of B-doped ZnO structures were modeled, as shown in Fig.1. A substitutional B-doped ZnO supercell was built by one boron atom substituting one zinc or oxygen atom, for interstitial B-doped ZnO, one boron atom was embedded in the interval of the tetrahedron or octahedron in ZnO lattice, they were labelled as $B_{s(Zn)}$, $B_{s(O)}$,$B_{i(tet)}$ and $B_{i(oct)}$ structure, respectively, as shown in Fig.1(b). All calculations were carried out using the CASTEP code based on DFT[23]. Electron-ion interactions were modeled by ultrasoft pseudopotentials[24], the Perdew-Wang generalized gradient approximation (GGA) was used as the exchange-correlation functional. The valence atomic configurations were $3d^{10}4s^2$ for Zn, $2s^22p^4$ for O, and $2s^22p^1$ for B, respectively, the wave functions of valence electrons were expanded by a plane-wave basis set with the cut-off energy of 420eV, the convergence threshold for self-consistent iterations was set at 5.0×10^{-7}eV/atom, k-point grid sampling in the supercells was set at 4×4×2. In the optimized process, the other parameters were set as follows: maximum force (0.01 eV/Å), maximum stress (0.02 GPa), changes in energy (5.0×10^{-6} eV/atom), and maximum displacement tolerance (5.0×10^{-4} Å).

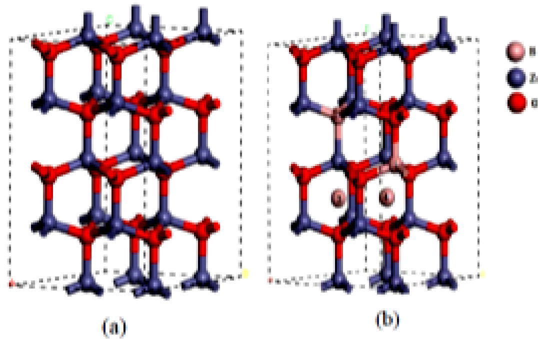

Fig.1. 2×2×2 supercell (a) ZnO, (b) B-doped ZnO, site 1 to 4 represents the boron replacements for B_s(Zn), B_s(O), $B_{i(tet)}$,$B_{i(oct)}$structure, respectively.

To describe the electronic and optical properties of B-doped ZnO accurately, the DFT+U method was adopted in this calculation, we set the U values of $U_{O,p}$=7.0eV for O 2p and $U_{Zn,d}$=10.5 eV for Zn 3d [25], by this way the calculated band-gaps and lattice constants for ZnO were consistent well with the experimental values[22].

3. Results and discussion

3.1. Structural properties

Table 1 listed the lattice constants, volume differences and bond lengths through optimizing the supercell of ZnO and four types of B-doped ZnO. In ZnO lattice, each zinc atom is bonded to one vertical and three horizontal oxygen atom, the average bond lengths were labeled as Zn-O_v and Zn-O_H , as were the bond lengths B-O_v and B-O_H for B-doped ZnO. The optimized lattice constants of ZnO are a=b=3.275Å, c=5.233Å, respectively, which are consistent well with the experimental values[22]. For $B_{s(Zn)}$ structure, the Zn-O_V and Zn-O_H bond lengths get larger than those of ZnO, the B-O_V and B-O_H bond lengths are 1.539Å and 1.523Å, respectively, which are shorter than those of Zn-O, which is attributed to the small radius of B^{3+} (0.27Å) compared to that of Zn^{2+} (0.74 Å), as a result, the cell volume of B_s(Zn) structure shrinks, which is well agreed with the other calculated value as well as experimental results[16,26]. For $B_{i(tet)}$ and $B_{i(oct)}$ structures, the Zn-O_H bond lengths near the interstitial B atoms are 2.871Å and 2.733 Å, respectively, which are much larger than the that of ZnO, therefore, the lattice constants (a and c) of B-doped ZnO for $B_{i(tet)}$ and $B_{i(oct)}$ structures increase, and the volume of cell expands by 7.4% and 4.8%, respectively.

Table 1. Optimized lattice constants, volume differences and bond lengths of ZnO and B-doped ZnO with different structure.

	a (Å)	c(Å)	ΔV (%)	Bond Lengths			
				Zn-O_H	Zn-O_V	B-O_H	B-O_V
ZnO	3.275, 3.249[a]	5.234 5.206[a]		1.989	2.001		
B_s(Zn)	3.233	5.181	-3.6, -3.1[b]	2.065, 1.996[b]	2.071	1.523,1.526[b]	1.539
B_s(O)	3.285	5.306	2.4	1.987			
B_i(tet)	3.292	5.434	7.4	2.871	2.131		
B_i(oct)	3.321	5.471	4.8	2.733	1.983		

a. Experimental values of reference [22]
b. Calculated values of reference [16]

3.2. Formation energy

The formation energies were used to determine the possibility of B-doped ZnO with different structures, which is expressed as the following [16, 27,28]:

$$E_f = E_t^{\text{Defect}} - E_t^{\text{ZnO}} + \sum n_i \mu_i \quad (1)$$

where E_t^{Defect} and E_t^{ZnO} are the total energies of B-doped ZnO and ZnO supercells, n_i is the number of i atoms, if the atom is added to the supercell, n_i is negative, otherwise it is positive, μ_i is the chemical potential of atom i. Formation energy is dependent on the growth condition, which may be Zn-rich or O-rich. As for ZnO, μ_{Zn} and μ_o satisfy the formula of $\mu_{Zn}+\mu_O=\mu_{ZnO}$. In O-rich condition, μ_O is determined by the total energy of O_2 molecules ($\mu_O = \mu_{O2}/2$), μ_{Zn} is calculated by the formula $\mu_{Zn}=\mu_{ZnO}-\mu_O$. In Zn-rich conditions, μ_{Zn} is the energy of one zinc atom in bulk zinc, μ_O is calculated by the formula $\mu_O=\mu_{ZnO}- \mu_{Zn(bulk)}$. μ_B is determined as follows: $\mu_B = (\mu_{B2O3} - 3\mu_O)/2$. From experimental point of view, chemical potentials have a wide range of values, therefore, in this work the formation energies of B-doped ZnO have values between those calculated in Zn-rich and O-rich conditions.

Table 2. Formation energies of four types of B-doped ZnO in Zn-rich and O-rich conditions.

Structure	Formation energy	
	Zn-rich	O-rich
$B_s(Zn)$	2.22	4.84
$B_s(O)$	7.35	20.48
$B_i(tet)$	5.24	13.12
$B_i(oct)$	6.71	14.58

Table 3. Formation energies and band-gaps of B-doped ZnO with different boron concentration.

Concentration	Formation energy(eV)		Band-gap (eV)	
	O-rich	Zn-rich		
Pure ZnO	--	--	3.36	0.91[b], 3.37[c]
6.25 at%	4.84 , 3.75[a]	2.22, 0.39[a]	3.15	0.87[b]
12.5 at%	10.46	5.21	3.07	
18.75 at%	16.33	8.45	2.99	

a. Calculated values of Ref.[16].
b. Calculated values of Ref.[14].
c. Experimental value of Ref.[22].

The calculated formation energies of four types of B-doped ZnO structure were summarized in Table 2. As we know, the defects having lower formation energy will form more easily. Under O-rich condition or under Zn-rich condition, the $E_f(B_i)$ and $E_f(B_s(O)$ are much larger than $E_f(B_s(Zn))$, indicating that boron doped into ZnO at the zinc site is much more easy than at oxygen site or the interstitial site of ZnO. Therefore, we used $B_s(Zn)$ structure for the following calculation and analyzed the properties of different concentration of B-doped ZnO. We used one, two and three boron atoms to substitute zinc atoms in 2×2×2 ZnO supercells, corresponding to doping levels of 6.2at.%, 12.5at.%, and 18.75at.%, respectively. Due to the same boron concentration having several supercell configurations, we have illustrated that the calculated results, such as the total energies and band gaps, varied in a small range with different configurations, and the average values were close to the values calculated by the configuration having large weight.

Table 3 listed the formation energies of B-doped ZnO with different boron concentration for $B_s(Zn)$ structure, the formation energies in Zn-rich condition is smaller than in O-rich condition for each boron concentration, which indicates Zn-rich growth condition facilitates Zn atoms to substitute boron atoms [16]. Furthermore, both in Zn-rich and in O-rich conditions, the formation energies increase with doping of boron, therefore, it would be difficult to prepare highly B-doped ZnO, because the larger formation energy is required.

3.3. Electronic structure

Fig. 2 shows the calculated band structures of pure ZnO and B-doped ZnO for $B_s(Zn)$ structure with different boron concentration, the Fermi energy is set to zero. The calculated band-gap for ZnO is 3.36eV, which is well consistent with the experimental value of 3.37eV, the direct band-gaps of B-doped ZnO with boron concentration at 6.25at.%, 12.5at.%,18.75at.% are 3.15eV, 3.07eV, 2.99eV, respectively. In addition, the Fermi energy shifts up into the conduction band for B-doped ZnO, indicating the characteristics of typical n-type conduction, as shown in Fig. 2(b), (c), (d). With boron doping ZnO becomes n-type conductor and its band-gap reduces, these results were also obtained by the calculations of Li Gao[14] and can be explained by the total and projected density of states (TDOS and PDOS) shown in Fig. 3.

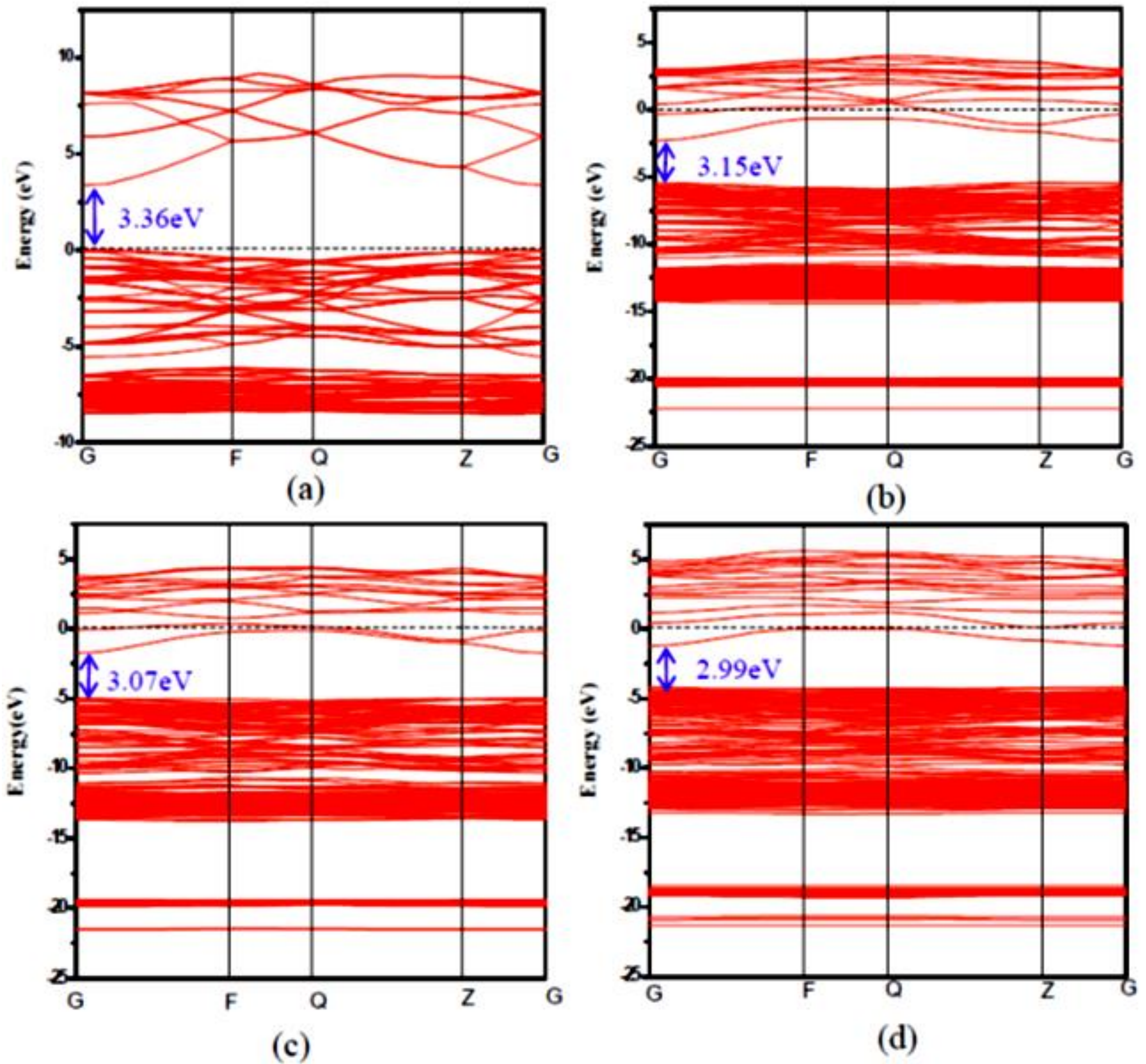

Fig. 2. Band structures of pure ZnO (a) and B-doped ZnO with boron concentration at 6.25at.% (b), 12.5at.% (c) and 18.75at.% (d). The Fermi energy is set to 0eV.

It can be seen in Fig. 3(a), for pure ZnO in the valence band (VB), the lower energy states (−9.2eV to −5.5eV) are mainly Zn-3d and O-2p orbitals, the upper states (−5.5eV to 0 eV) are mainly the O-2p orbital, the conduction band (CB) is dominated by Zn-4s and Zn-4p states, hybridized with some O-2s and O-2p orbitals [29], following the substitution of one zinc atom by one boron atom, the CB divides the lower (-1.8eV to 0.7eV) and upper (0.7eV to 5.4eV) energy states as shown in Fig. 3(b), the two region mainly comprises Zn-4s and Zn-4p as well as some O-2p and B-2p orbitals, the electrons occupying the lower region result in the Fermi energy(set to zero and marked by dot line) moving upward into the CB, indicating the characteristic of typical *n*-type semiconductor. In addition, it can be seen in Fig. 3(a), for pure ZnO the conduction band minimum(CBM) is the hybridization of the orbitals of Zn-4s,-4p and O-2s,-2p, with boron doping the hybridization of the orbitals for the CBM is added to B-2s,2p as shown in Fig. 3(b), the orbital of B-2s locate in lower energy position, resulting in a decrease of the energy band gap.

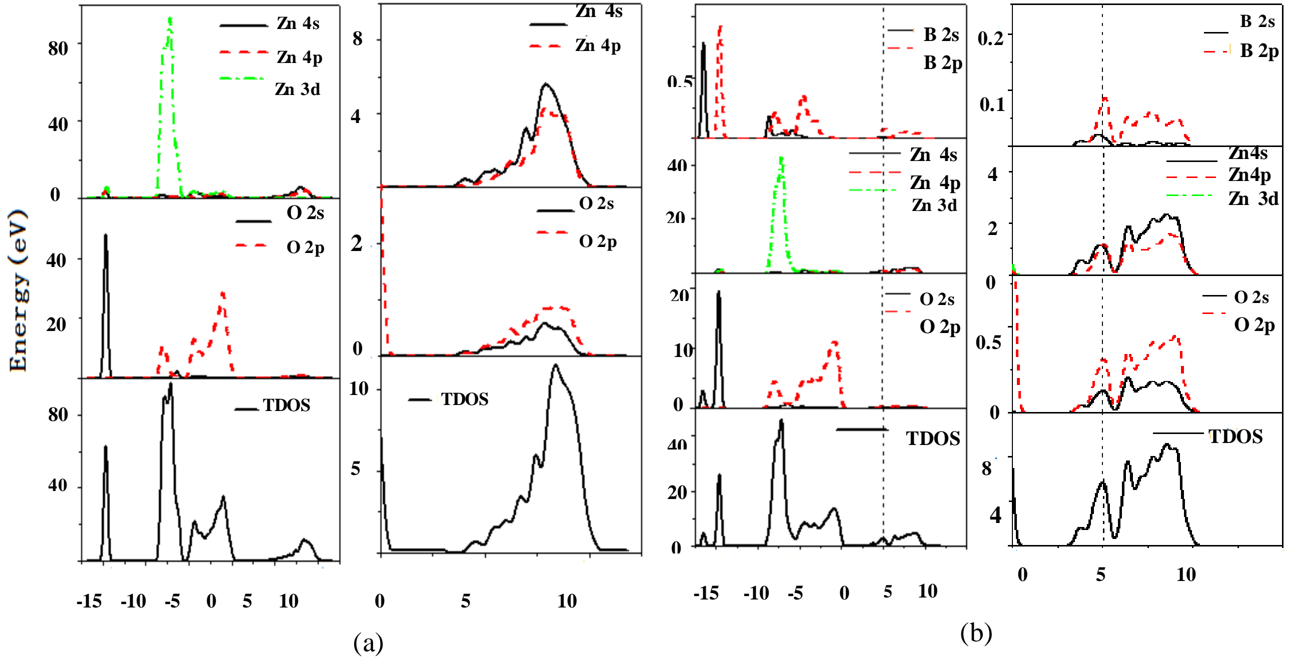

Fig. 3. Density of state for (a) pure ZnO, (b) B-doped ZnO with boron concentration at 6.25at.% .

3.4. Optical properties

The optical properties of a material can be described by dielectric function ε(ω)=ε1(ω)+iε2(ω), in this function ε1(ω) and ε2(ω) are the real and imaginary part, which can be calculated according to the Kramers–Kronig's dispersion relation[30]. In this way, other optical properties, such as absorption coefficient α(ω), reflectivity R(ω) can also be acquired. The related formulas are listed as below.

$$\varepsilon_2(\omega)=\frac{2e^2\pi}{\Omega\varepsilon_0}\sum_{k,c,v}\left|\left\langle\varphi_c^k\left|u\cdot r\right|\varphi_v^k\right\rangle\right|^2\delta(E_c^k-E_v^k-\omega) \tag{2}$$

$$\varepsilon_1(\omega)=1+\frac{2}{\pi}\rho_0\int_0^\infty\frac{\omega'\varepsilon_2(\omega)}{\omega'^2-\omega^2}d\omega' \tag{3}$$

$$\alpha(\omega)=\sqrt{2}\left[\sqrt{\varepsilon_1^2(\omega)+\varepsilon_2^2(\omega)}-\varepsilon_1(\omega)\right]^{1/2} \tag{4}$$

$$R(\omega)=\left|\frac{\sqrt{\varepsilon(\omega)}-1}{\sqrt{\varepsilon(\omega)}+1}\right|^2 \tag{5}$$

where, Ω is the volume of unit cell, e is the electronic charge, u is the vector of electric field defining the polarization, ω is the frequency of incident light; and φ_c^k and φ_v^k are the wave functions of valence and conduction band, E_c^k and E_c^k are the intrinsic energy, respectively.

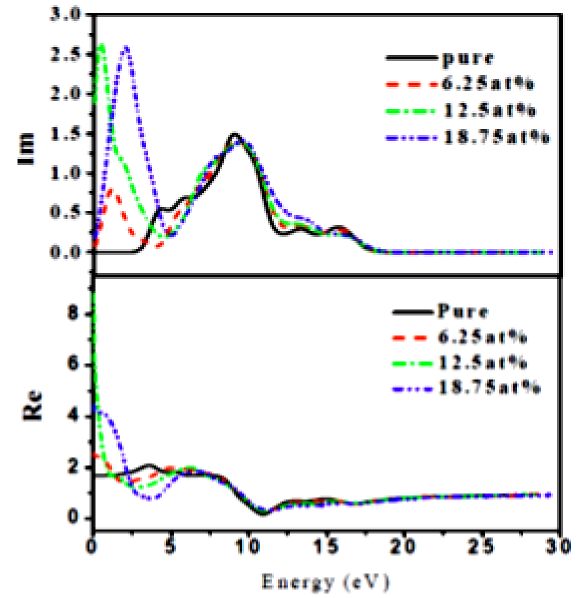

Fig. 4. Dielectric function of pure ZnO, B-doped ZnO with different boron concentration.

Fig. 4 shows the dielectric function of B-doped ZnO with different boron concentration. In the range of

5eV-30eV, the trends of imaginary and real part are much similar for B-doped ZnO with various boron concentration. While in the range of 0eV-5eV, the imaginary part increases with boron concentration increasing, and the peak has the offset to the smaller energy side. It can be found that the real part decreases successively with boron concentration increasing in the range of 3eV-5eV.

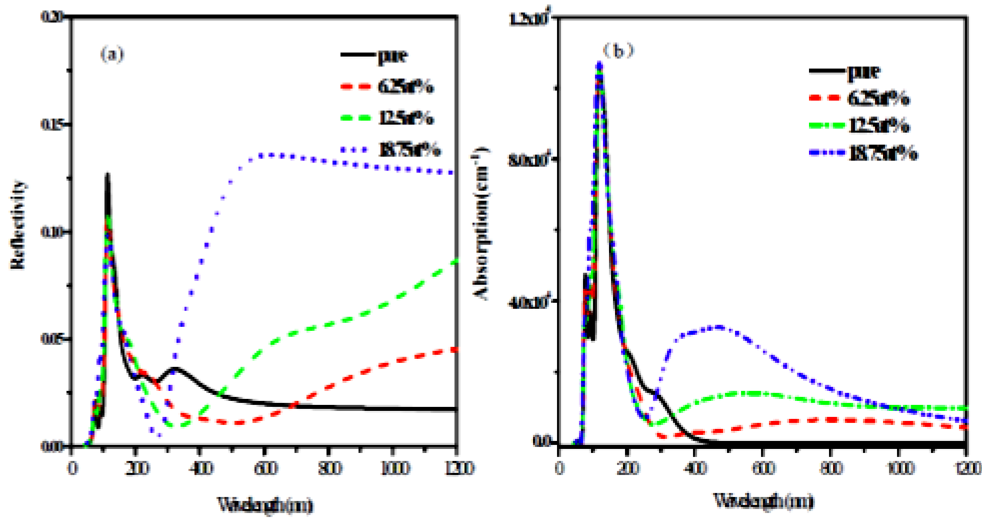

Fig. 5. (a) Reflectivity, and (b) Absorption of pure ZnO and B doped ZnO with different boron concentration.

Fig. 5 shows the reflectivity and absorption spectra of B-doped ZnO with different boron concentration. As boron concentration increases from 0 to 18.75at.%, the reflectivity decreases at short wavelength (200nm-300nm) while increasing at long wavelength. The transforming wavelength has blue shift with the incorporation of boron, as shown in Fig. 5(a). Compared with pure ZnO, the absorption decreases obviously in the high energy range of 200-300nm after doping, while in the wavelength of 300-1200nm, the absorption increases significantly with boron concentration increasing, especially in the range of 300-800nm. While in the ultraviolet of 0-300nn, the reflectivity and absorption almost has the same trend with B-doping, which is consistent with the dielectric function in Fig. 4.

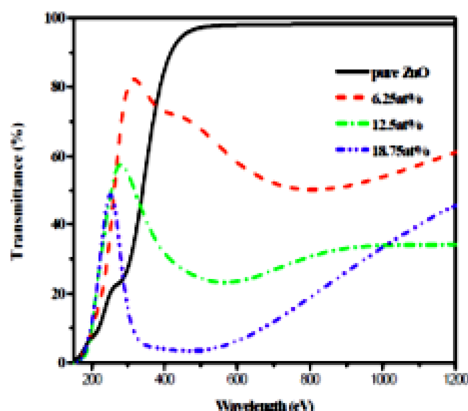

Fig. 6. The calculated transmittance spectra of B-doped ZnO with different boron concentration.

Fig. 6 shows the calculated transmittance for pure ZnO and B-doped ZnO with different boron concentration. In the range of 400nm-1200nm, the average transmittance of ZnO is larger than 90%, which complies well with the experimental results by Li Gao et al.[14], they deposited ZnO thin films by RF magnetron sputtering which have a transmittance of over 95% in the wavelength range from 720nm to 800nm, over 95% transmittance were also observed in ZnO films by R. Ondo-Ndong et al. and C. Wang et al. [31,32]. Following the incorporation of boron, the transmittance decreases, while at low concentration (6.25at%) the average transmittance is still larger than 60%, which is also consistent with the experimental results[14] and other theoretical calculation[16]. In the ultraviolet (UV) region (200nm-400nm), the main peaks shift toward short wavelength with boron concentration increasing, at wavelength shorter than 300nm, the transmittance of B-doped ZnO is higher than that for pure ZnO, however, the transmittance decreases with boron concentration increasing. For boron concentration between 6.2at.% and 18.25at.% and in the range of 400nm-1200nm, the transmittance decreasing is similar to that of Al or Ga-doped ZnO, which was considered to be due to the number of donor states increasing [33,34].

4. Conclusion

In this study, we employed DFT+U to investigate the electronic and optical properties of B-doped ZnO, $U_{o,p}$ = 7eV for O 2p and $U_{Zn,d}$ = 10.5eV for Zn 3d were set as the Hubbard U values. Four B-doped ZnO structures were considered in this calculation, they were the

substitution of boron for zinc ($B_{s(Zn)}$) or oxygen ($B_{s(O)}$), the interstitial boron in a tetrahedron ($B_{i(tet)}$) or in an octahedron ($B_{i(oct)}$). The calculated formation energies indicated that $B_{s(Zn)}$ structure forms easily compared to the other three structures, and it is difficult to prepare B-doped ZnO with high doping level. For $B_{s(Zn)}$ structure with different boron concentration, the Fermi energy shifts into the conduction band, indicating the characteristics of typical n-type semiconductor, in addition, the band-gap decreases with boron concentration increasing, they are 3.15eV, 3.07eV, 2.99eV with boron concentration at 6.25at%, 12.5at%, 18.75at%, respectively. The optical properties of B-doped ZnO for $B_{s(Zn)}$ structure were also calculated at different boron concentration. In the range of 400nm-1200nm, the average transmittance of ZnO is lager than 90%, the transmittance decreases following the incorporation of boron, at low concentration (6.25at%) the average transmittance is larger than 60%, at wavelength shorter than 300nm, the transmittance of B-doped ZnO is larger than that of ZnO. These characteristics are similar to Al or Ga-doped ZnO on optical properties.

Acknowledgements

This work was supported by Science and Technology Planning Project of Guangzhou city (2016201604030035 and 201604016095), Science and Technology Planning Project of Guangdong Province (2015B010112002), Science and Technology Planning Project of Zhongshan city (2017A1008). We also acknowledge R&D Center for Semiconductor Lighting of Chinese Academy of Sciences providing us the use of CASTEP simulation program.

References

[1] E. Fortunato, P. Nunes, D. Costa, D. Brida, I. Ferreira, R. Martins, Vacuum **64**, 233 (2002).
[2] P. H.Lei, M. J. Ding, Y. C. Lee, M. J. Chung, J. Alloys Compd. **509**, 6152 (2011).
[3] H. H.Huang, S. Y. Chu, P. C. Kao, Y. C. Chen, M. R. Yang, Z. L. Tseng, J. Alloys Compd. **479**, 520 (2009).
[4] J. Muller, G. Schope, O. Kluth, B. Rech, M. Ruske, J. Trube, B. Szyszka, X. Jiang, G. Brauer, Thin Solid Films **392**, 327 (2001).
[5] Z. Z. You, G. J. Hua, J. Alloys Compd.**530**, 11 (2012).
[6] Q. Zhang, C. S. Dandeneau, X. Zhou, G. Cao, Adv. Mater. **21**, 4087 (2009).
[7] M. Selmi, F. Chaabouni, M. Abaab, B. Rezig, Superlattices and Microstructures **44**, 268 (2008).
[8] W. W. Wang, X. G. Diao, Z. Wang, M. Yang, T. M. Wang, Z. Wu, Thin Solid Films **491**, 54 (2005).
[9] P. Li, S. H. Deng, L. Zhang, Y. B. Li, J. Y. Yu, D. Liu, Chin. J. Chem. Phys. **23**, 527 (2010).
[10] A. Stashans, K. Olivos, R. Rivera, Phys. Scr. **83**, 065604 (2011).
[11] M. Bazzani, A. Neroni, A. Calzolari, A. Catellani, Appl. Phys. Lett. **98**, 121907 (2011)
[12] C. Y. Tsay, K. S. Fan, C. M. Lei, J. Alloys Compd. **512**, 216 (2012).
[13] S. Peng, Y. K. Tang, L. M. Jin, Y. Wang, L. Y. Ma, F. F. Cao, Surface & Coatings Technology **310**, 251 (2017).
[14] L. Gao, Y. Zhang, J. M. Zhang, K. W. Xu, Appl. Surf. Sci. **257**, 2498 (2011).
[15] Y. F. Wang, H. Y. Huang, X. D. Meng, F. Yang, J. Y. Nan, Q. G. Song, J. Alloys Comp. **636**, 102 (2015).
[16] Y. C.Peng, C. C. Chen, H. C. Wu, J. H. Lu, Optical Materials **39**, 34 (2015).
[17] H. C. Wu, Y. C. Peng, C. C. Chen, Optical Materials **35**, 509 (2013).
[18] C. Y. Ren, S. H. Chiou, C. S. Hsue, Physica B **349**, 136 (2004).
[19] R. W. Godby, M. Schluter, L. J. Sham, Phys. Rev. B **36**, 6497 (1987).
[20] X. Ma, Y. Wu, Y. Lu, J. Xu, Y. Wang, Y. Zhu, J. Phys.Chem. C **115**, 16963 (2011).
[21] X. Ma, B. Lu, D. Li, R. Shi, C. Pan, Y. Zhu, J. Phys.Chem. C **115**, 4680 (2011).
[22] R. D. Vispute, V. Talyansky, S. Choopun, R. P. Sharma, T. Venkatesan, M. He, Appl. Phys. Lett. **73**, 348 (1998).
[23] M. D. Segall, J. D. Lindan, M. J. Probert, C. J. Pickard, P. J. Hasnip, S. J. Clark, J. Phys. Condens. Matter **14**, 2717 (2002).
[24] D. Vanderbilt, Phys. Rev. B **41**, 7892 (1990).
[25] R. M. Sheetz, I. Ponomareva, E. Richter, A. N. Andriotis, M. Menon, Phys. Rev. B **80**, 195314 (2009).
[26] X. G. Xu, H. L. Yang, Y. Wu, D. L. Zhang, S. Z. Wu, Appl. Phys. Lett. **97**, 232502 (2010).
[27] A. Janotti, C. G. Van de Walle, Phys. Rev. B: Condens. Matter. **76**, 165202 (2007).
[28] T. Guo, G. Dong, Q. Chen, X. Diao, F. Gao, J. Phys. Chem. Solids **75**, 42 (2014).
[29] F. Oba, M. Choi, A. Togo, I. Tanaka, Sci. Technol, Adv. Mater. **12**, 034302 (2011).
[30] X. C. Liu, Y. J. Ji, J. Q. Zhao, L. Q. Liu, Z. P. Sun, H. L. Dong, Acta Physico-Chimica Sinica **59**, 4925 (2010).
[31] R. Ondo-Ndong, G. Ferblantier, M. Al. Kalfioui, A. Boyer, A. Foucaran, J. Cryst. Growth **255**, 130 (2003).
[32] C. Wang, Z. G. Ji, J. H. Xi, J. Du, Z. Z. Ye, Mater. Lett. **60**, 912 (2006).
[33] M. Bazzani, A. Neroni, A. Calzolari, A. Catellani, Appl. Phys. Lett. **98**, 121907 (2011).
[34] S. Y. Lee, Y. C. Peng, J. H. Lu, Y. R. Zhu, H. C. Wu, Thin solid films **570**, 460 (2014).

*Corresponding author: depingxiong@gdut.edu.cn